Anomaly Detection of Hyperspectral Imagery Using Differential Morphological Profile

Ashkan Taghipour
Faculty of Electrical and Computer
Engineering, Tarbiat Modares
University,Tehran, Iran
ashkan.taghipour@modares.ac.ir

Hassan Ghassemian
Faculty of Electrical and Computer
Engineering, Tarbiat Modares
University, Tehran, Iran
ghassemi@modares.ac.ir

Fardin Mirzapour
Faculty of Electrical and Computer
Engineering, Tarbiat Modares
University, Tehran, Iran
f.mirzapour@modares.ac.ir

Abstract—**Anomaly detection has been an interesting topic in hyperspectral imagery. Most anomaly detection methods use spectral information for detecting targets. In this paper we propose a method which uses both spectral and spatial information for detecting anomalies: differential morphological profile anomaly detection (DMPAD). This method utilizes principal component analysis (PCA) and differential morphological profile (DMP) to extract spectral and spatial information from hyperspectral image (HSI), respectively. The experimental results confirm DMPAD method's superiority to three mostly used anomaly detection methods, namely PCA, fisher linear discriminant (FLD) and Reed-Xiaoli (RX) methods. DMPAD detects more accurate targets and less false alarm in comparison with competing method.**

Keywords-component; anomaly detection; differential morphology; hyperspectral imagery;

I. INTRODUCTION

Remotely sensed hyperspectral imagery is of interest due to its capability to extract valuable information from objects or scenes located on the earth surface [1]. One of the most attractive topics in remote sensing is target detection. In remote sensing, target is not a specific object; It is considered whatever has specific feature like certain spectra or something that has considerable different from its background. Target detection methods in hyperspectral imagery, can be categorized into two main classes [2]: 1) signature matching-based [3] 2) anomaly detection [4]. In signature matching-based methods, a priori knowledge about target spectra is essential for detection and that spectra can be obtained from a spectral library or, by applying spectral matched filters on training data samples [5], however in anomaly detection no *a priori* information about target spectra is needed. Generally speaking, anomaly detectors try to locate whatever looks spatially or spectrally different from its neighborhood [5]. Anomaly detection has been alluring topic in hyperspectral imagery due to its wide applications such as detecting location of crop stress in precision farming, finding scarce minerals in geology, oil and environmental pollution analysis, detecting landmines for public safety, and military applications [6], [7]. Due to the diversity of these applications, different methods have been proposed. One of the most popular methods is Reed-Xiaoli (RX) which has been considered as the benchmark for performance evaluation of hyperspectral anomaly detectors [1], [8]. Even though RX anomaly detector has been extensively used, it faces some problems due to assumption about its background density function. RX detector considers multivariate normal distribution for background density function, which does not hold in many scenarios because local background can be too complex to be characterized by a multivariate normal distribution [2]. Another well-known method in anomaly detection is principal component analysis (PCA) [9]. Fisher linear discriminant (FLD) is another method which is used in anomaly detection. By defining between-class and within-class scatter matrices, FLD tries to produce a projection separation so that the between-class distance is maximize and the within-class distance is minimize [5].

It is worthwhile to mention that all aforementioned anomaly detection methods are based on spectral information of scenes, whereas using spatial features can give us valuable information about anomalies. The use of spatial information in hyperspectral image analysis have been extensively used in [10-12]. We propose derivative morphological profile anomaly detection (DMPAD) method which utilizes both spectral and spatial information of hyperspectral data to detect anomalies. In DMPAD, we use PCA for extracting spectral information, and differential morphological profile (DMP) for spatial features extraction. It is noteworthy that both PCA and DMP are fast and easy-to-implement operations. In this paper we use San Diego airport hyperspectral image for evaluating our proposed method.

The remainder of this paper is organized in the following manner. Section II represents a brief overview of the mostly utilized anomaly detection methods. Section III introduces the proposed method. Experimental results and conclusion are represented in Section IV and V respectively.

II. RELATED WORKS

In this section we will have a brief overview on three most popular anomaly detection methods: RX, PCA and FLD. It is noteworthy that most anomaly detection methods are based on dual-window approach [8]. Inner window region (IWR) and outer window region (OWR) shown in Fig. 1.The inner window size is selected so that it can surround the biggest target, so we need some *a priori* information about the size of the targets of interest. To avoid mixing the statistics of IWR and OWR, using a guard window which is slightly larger than inner window size, has been considered.
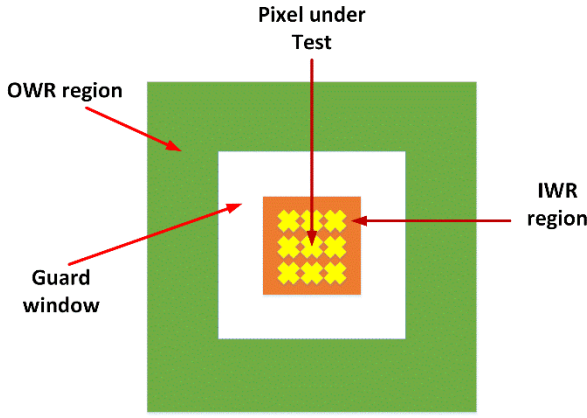
Fig. 1. An example of dual concentric window with guard band

It is remarkable to mention that we did not use dual window approach directly in the proposed methods, though, we use the concept for choosing the size of morphological filters.

A. Reed-Xiaoli

The RX detector has been introduced by Reed and Yu [13]. RX detector is considered as the benchmark for hyperspectral anomaly detection because it considers spectrum of targets as unknown and the background covariance matrix, as well. RX detector is the square of Mahalanobis distance and is given by

$$\mathbf{RX}(\mathbf{r}) = (\mathbf{r} - \boldsymbol{\mu}_{\text{out}})^T \mathbf{C}_{\text{out}}^{-1} (\mathbf{r} - \boldsymbol{\mu}_{\text{out}}) \qquad (1)$$

where $\mathbf{r}$ is the pixel under test, $\boldsymbol{\mu}_{\text{out}}$ and $\mathbf{C}_{\text{out}}^{-1}$ are spectral mean vector and spectral covariance matrix of the outer window around the pixels, respectively.

B. Principal Component Analysis

Applying PCA transform on hyperspectral data is one of the most popular methods which is used in dimensionality reduction [14] and feature extraction[15],[16]. PCA by minimizing the mean square error (MSE) of represented signal produces uncorrelated features. The Utilize of PCA transform in anomaly detection have been presented in [5]. Related PCA equations is as follows

$$\mathbf{C}_{\text{out}} = \mathbf{V} \boldsymbol{\Lambda} \mathbf{V} \qquad (2)$$

aforementioned equation represents covariance matrix of outer window in terms of its eigenvectors $\mathbf{V}$ and eigenvalues $\boldsymbol{\Lambda}$. By choosing m first eigenvectors which relates to most eigenvalues, we have

$$\mathbf{B}_{\text{PCA}} = \widetilde{\mathbf{V}} = [\mathbf{v}_1, \mathbf{v}_2, \ldots, \mathbf{v}_m] \qquad (3)$$

where m is an adjustable constant which can be altered and has direct influence on performance of anomaly detector.
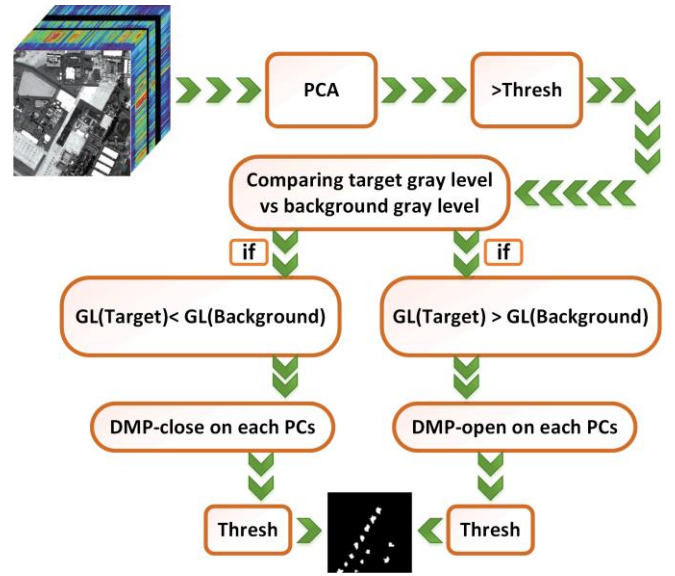

Fig 2. Flowchart of DMPAD method

Finally the PCA anomaly detector is given by

$$\mathbf{PCA}(\mathbf{r}) = (\mathbf{r} - \boldsymbol{\mu}_{\text{out}})^T (\mathbf{B}_{\text{PCA}} \mathbf{B}_{\text{PCA}}^T)(\mathbf{r} - \boldsymbol{\mu}_{\text{out}}) \qquad (4)$$

Aforementioned equation can be implemented by inner window too, just $\mathbf{B}_{\text{PCA}}$ will be corresponding eigenvectors of inner window covariance matrix and $\boldsymbol{\mu}_{\text{out}}$ should replace with $\boldsymbol{\mu}_{\text{in}}$. In this paper results are based on outer window which shows better result than inner window

C. Fisher Linear Discriminant

In spite of RX and PCA methods, which did not consider information of inner window and outer window simultaneously, FLD utilizes IWR and OWR data by defining between-class scatter matrix $\mathbf{S}_B = (\boldsymbol{\mu}_{\text{in}} - \boldsymbol{\mu}_{\text{out}})(\boldsymbol{\mu}_{\text{in}} - \boldsymbol{\mu}_{\text{out}})^T$ and within-class scatter matrix $\mathbf{S}_{\text{tot}} = \mathbf{C}_{\text{out}} + \mathbf{C}_{\text{in}}$ represented in detail in [5] where $\mathbf{C}_{\text{in}}$ and $\mathbf{C}_{\text{out}}$ are corresponding covariance matrices of inner and outer window. The FLD anomaly detector given by

$$\mathbf{FLD}(\mathbf{r}) = (\mathbf{r} - \boldsymbol{\mu}_{\text{out}})^T (\mathbf{B}_{\text{FLD}}^* (\mathbf{B}_{\text{FLD}}^*)^T)(\mathbf{r} - \boldsymbol{\mu}_{\text{out}}) \qquad (5)$$

where $\mathbf{B}_{\text{FLD}}^* = \mathbf{S}_{\text{tot}}^{-1}(\boldsymbol{\mu}_{\text{in}} - \boldsymbol{\mu}_{\text{out}})$ which extract from equation below

$$\mathbf{B}_{\text{FLD}}^* = \max_{\mathbf{B}_{\text{FLD}}} J(\mathbf{B}_{\text{FLD}}) = \frac{|\mathbf{B}_{\text{FLD}}^T \mathbf{S}_B \mathbf{B}_{\text{FLD}}|}{|\mathbf{B}_{\text{FLD}}^T \mathbf{S}_{\text{tot}} \mathbf{B}_{\text{FLD}}|} \qquad (6)$$

which tries to maximize between-class separation and minimize within-class compactness.

I. PROPOSED METHOD

In this section we introduce our propose anomaly detection method, which is called DMPAD. The flowchart of DMPAD

Fig. 3. Nineteenth band of Hyperspectral image and region under test

algorithm has been shown in Fig. 2. The description of DMPAD is represented in detail as follows:

1- At first, we do a PCA on hyperspectral data. The number of Principal Components (PCs) are selected based on main component which have more than 99.9% information (energy) of Hyperspectral data. In our experiments, ten PCs are selected. The use of this step help us to utilize spectral information of data, also it reduces complexity of algorithm because of reduction in dimension of data.

2- After applying PCA, we put a high threshold on summation of all PCs, for detection of target candidates. See Fig. 2. Putting high threshold causes accessing reliable target candidates. Extracting reliable target candidates can lead us to more accurate post processing steps

3- In this step, we will obtain a target map which can be used for finding target pixels location and can be utilized for comparing target candidates gray level with their background gray level. For comparison, a window (which surround the target candidates and contain three times more pixels than target candidates pixels) considers and gray level mean of target candidates compares with gray level mean of its background.

4- After aforementioned comparison, differential morphological profile by opening reconstruction (DMPO) or differential morphological profile by closing reconstruction (DMPC), adaptively will choose, for applying on each PC. Adaptively means that if gray level mean of target candidates is more than gray level mean of its background, (due to inherent morphological filter features) the use of DMPO is suggested and will choose automatically, and if gray level mean of target candidates is less than gray level mean of its background, the use of DMPC is proposed. So, this method by using simple comparison between gray level mean of target candidates and background, adaptively diagnoses which branch (DMPO or DMPC) should be implement on each PC. DMP has been represented in detail in [17], and we have brought a brief overview of it.

DMP can be implemented either with opening by reconstruction or closing by reconstruction. Opening by reconstruction can be implemented by an erosion with the Structure Element (SE) and follows reconstruction by a dilation. We denote opening by reconstruction with $\omega_R^i(g)$ that i is SE size, R comes from reconstruction and g is an image which opening by reconstruction applies on it. With respect to duality, we have $\delta_R^i(g)$ which is closing by reconstruction and defined as the dilation of the image with specific SE size that follows a reconstruction by an erosion. The opening morphological profile, formulized as follows

$$\Omega_{\omega R}(g) = \{\Omega_{\omega i} : \Omega_{\omega i} = \omega_R^i(g), \forall i \epsilon [0, \dots, n]\} \qquad (7)$$

in a similar way for closing morphological profile we have

$$\Omega_{\delta R}(g) = \{\Omega_{\delta i} : \Omega_{\delta i} = \delta_R^i(g), \forall i \epsilon [0, \dots, n]\} \qquad (8)$$

so, DMP can be defined

$$\Delta_{\omega R}(g) = \{\Delta_{\omega i} : \Delta_{\omega i} = \Omega_{\omega(i-1)} - \Omega_{\omega i}, \forall i \epsilon [1, n]\} \qquad (9)$$

$$\Delta_{\delta R}(g) = \{\Delta_{\delta i} : \Delta_{\delta i} = \Omega_{\delta(i-1)} - \Omega_{\delta i}, \forall i \epsilon [1, n]\} \qquad (10)$$

where (9) is DMPO and (10) is DMPC. In this step we implement the DMPO or DMPC on each PC and summation of them considers as final target map.

5- Finally, by putting a threshold, binary target map obtains.

II. EXPERIMENTAL RESULTS

In this section, we bring our proposed method results, furthermore we compare our results with three method which are PCA, FLD and RX. The hyperspectral image has been used in our experiments is part of San Diego airport in USA. It has 189 spectral bands and spatial resolution of 3.5 m, we do our experiments on 80×80 region of that. Nineteenth band of San Diego hyperspectral data and region under test is shown in Fig. 3. For implementation DMPAD method, we consider line and square with dimension of 2 and 8×8, respectively as SEs. The reason for choosing line and square is inherent feature of DMP which gives us residues of two successive filtering operation [8] and when we consider line as a filter more residues that means better target surface, extracts and has considered as anomaly. We examine three sets of filter for SEs that were line-square, line-disk and disk-square and as we expected, line-square and line disk had better results in comparison with disk-square, because less residues remain when we subtract disk and square from each other. Experimental results shows better performance when we use line-square as SEs with aforementioned sizes. For selecting dimension of windows we follow a similar approach like dual-window. We choose square filter SE size in a way that surround the biggest target and line filter 2 for much more residues. It is worthwhile to mention that the degree of line SE has negligible effect on detecting anomalies and we consider it 0. Fig. 4 represents implementation results of different anomaly detection methods on San Diego hyperspectral image.
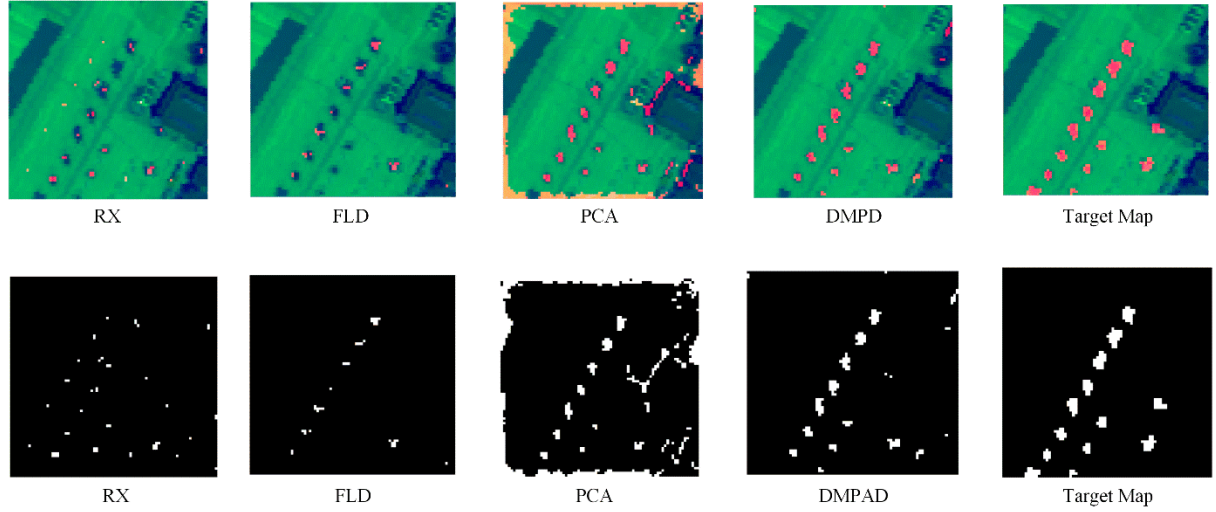
Fig. 4. Simulation results of different methods. Top are false color of detection results and bottom are binary results
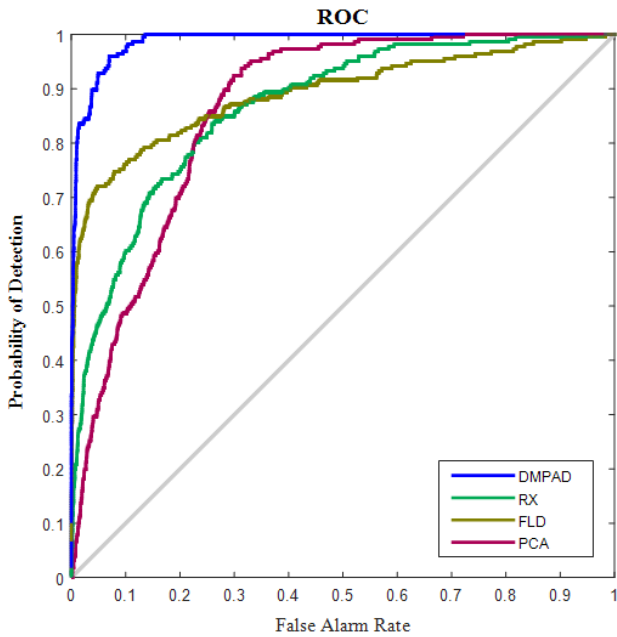

Fig. 5. ROC curve of different methods

As can be seen from Fig. 4, the proposed method shows better performance in comparison with three other methods. results show that PCA method has not acceptable performance in margin of the image, FLD method detects less target than DMPAD and RX detects more false alarm in comparison with aforementioned method. Actually DMPAD method detects more accurate targets and also it has less false alarm in comparison with three others. In Fig. 5, the receiver operation characteristics (ROC) curve, which illustrates probability of detection versus probability of false alarm has been plotted. ROC curve is a mean to evaluate performance of detector

independent from selecting threshold η. As can be seen, proposed method (DMPAD) shows better detection probability in specific false alarm.

III. CONCLUSION

We proposed DMPAD method for anomaly detection in hyperspectral imagery. Different from well-known anomaly detection methods which utilizes spectral information of hyperspectral image, DMPAD uses both spectral and spatial features of the scene for detecting anomalies. We suggested differential morphological profile for extracting spatial features and PCA for extracting spectral information of the scene. We compared DMPAD with three well-known methods; RX, PCA and FLD. Experimental results proved superiority of DMPAD method to competing methods. DMPAD method could detect more accurate targets. Also it provoked less false alarms in comparison with three others.

REFERENCES

[1] J. M. Bioucas-Dias, A. Plaza, G. Camps-Valls, P. Scheunders, N. M. Nasrabadi, and J. Chanussot, "Hyperspectral Remote Sensing Data Analysis and Future Challenges," *IEEE Geoscience and Remote Sensing Mag.,* vol. 1, no. 2, pp. 6-36, 2013.

[2] G. Qiandong, Z. Bing, R. Qiong, G. Lianru, L. Jun, and A. Plaza, "Weighted-RXD and Linear Filter-Based RXD: Improving Background Statistics Estimation for Anomaly Detection in Hyperspectral Imagery," *IEEE J. Select. Topics Appl. Earth Observ. Remote Sensing,* vol. 7, no. 6, pp. 2351-2366, 2014.

[3] Z. Zhengxia and S. Zhenwei, "Hierarchical Suppression Method for Hyperspectral Target Detection," *IEEE Trans. Geosci. Remote Sensing,* vol. 54, no. 1 , pp. 330-342, Jan. 2016.

[4] Y. Yuan, D. Ma, and Q. Wang, "Hyperspectral Anomaly Detection by Graph Pixel Selection," *IEEE Trans. on Cybernetics,* In Press.

[5] K. Heesung and N. M. Nasrabadi, "Kernel RX-algorithm: a nonlinear anomaly detector for hyperspectral imagery," *IEEE Trans. Geosci. Remote Sensing,* vol. 43, no. 2, pp. 388-397, 2005.

[6] L. Jiayi, Z. Hongyan, Z. Liangpei, and M. Li, "Hyperspectral Anomaly Detection by the Use of Background Joint Sparse Representation," *IEEE J. Select. Topics Appl. Earth Observ. Remote Sensing,* vol. 8, no. 6, pp. 2523-2533, 2015.

[7] R. Zhao, B. Du, L. Zhang, and L. Zhang, "Beyond Background Feature Extraction: An Anomaly Detection Algorithm Inspired by Slowly Varying Signal Analysis," *IEEE Trans. Geosci. Remote Sensing,* In Press.

[8] N. M. Nasrabadi, "Hyperspectral Target Detection : An Overview of Current and Future Challenges," *IEEE Signal Processing Mag.,* vol. 31, no. 1, pp. 34-44, 2014.

[9] H. Goldberg and N. M. Nasrabadi, "A comparative study of linear and nonlinear anomaly detectors for hyperspectral imagery," in *Proc. SPIE,* 2007, pp. 656504-656504-17.

[10] M. Golipour, H. Ghassemian, and F. Mirzapour, "Integrating Hierarchical Segmentation Maps With MRF Prior for Classification of Hyperspectral Images in a Bayesian Framework," *IEEE Trans. Geosci. Remote Sensing,* In Press.

[11] M. Borhani and H. Ghassemian, "Kernel Multivariate Spectral-Spatial Analysis of Hyperspectral Data," *IEEE J. Select. Topics Appl. Earth Observ. Remote Sensing,* vol. 8, no. 6, pp. 2418-2426, 2015.

[12] F. Mirzapour and H. Ghassemian, "Improving hyperspectral image classification by combining spectral, texture, and shape features," *International Journal of Remote Sensing,* vol. 36, pp. 1070-1096, 2015/02/16 2015.

[13] L. Wei and D. Qian, "Collaborative Representation for Hyperspectral Anomaly Detection," *IEEE Trans. Geosci. Remote Sensing,* vol. 53, no. 3, pp. 1463-1474, 2015.

[14] J. Zabalza, R. Jinchang, Z. Jiangbin, H. Junwei, Z. Huimin, L. Shutao*, et al.*, "Novel Two-Dimensional Singular Spectrum Analysis for Effective Feature Extraction and Data Classification in Hyperspectral Imaging," *IEEE Trans. Geosci. Remote Sensing,* vol. 53, no. 8, pp. 4418-4433, 2015.

[15] M. Imani and H. Ghassemian, "Feature Extraction Using Weighted Training Samples," *IEEE Geosci. Remote Sensing Lett.,* vol. 12, no. 7, pp. 1387-1391, 2015.

[16] M. Imani and H. Ghassemian, "Band Clustering-Based Feature Extraction for Classification of Hyperspectral Images Using Limited Training Samples," *IEEE Geosci. Remote Sensing Lett., IEEE,* vol. 11, no. 8, pp. 1325-1329, 2014.

[17] M. Dalla Mura, J. A. Benediktsson, B. Waske, and L. Bruzzone, "Morphological Attribute Profiles for the Analysis of Very High Resolution Images," *IEEE Trans. Geosci. Remote Sensing,* vol. 48, no. 10, pp. 3747-3762, 2010.